Inorganic Chemistry

pubs.acs.org/IC

Communication

Rhenium Biscorrole Sandwich Compounds: XAS Evidence for a New Coordination Motif

Abraham B. Alemayehu, Macon Jedediah Abernathy, Jeanet Conradie, Ritimukta Sarangi,* and Abhik Ghosh*

Cite This: *Inorg. Chem.* 2023, 62, 8467−8471

Read Online

ACCESS | Metrics & More | Article Recommendations | Supporting Information

ABSTRACT: The interaction of three free-base *meso*-tris(*p*-X-phenyl)corroles H_3[T*p*XPC] (X = H, CH_3, OCH_3) with $Re_2(CO)_{10}$ at 235 °C in the presence of K_2CO_3 in *o*-dichlorobenzene has led to putative rhenium biscorrole sandwich compounds with the formula ReH[T*p*XPC]$_2$. Density functional theory calculations and Re L_3-edge extended X-ray absorption fine structure measurements suggest a seven-coordinate metal center, with the "extra" hydrogen located on one of the corrole nitrogens. The complexes can be deprotonated by a base such as 1,8-diazabicyclo[5.4.0]undec-7-ene, resulting in a substantial sharpening of the UV−vis spectra and split Soret bands, consistent with the generation of C_2-symmetric anions. Both the seven-coordinate neutral and eight-coordinate anionic forms of the complexes represent a new coordination motif in the field of rhenium−porphyrinoid interactions.

The interaction of rhenium with porphyrin-type ligands has resulted in a growing variety of coordination motifs in recent years.[1,2] Thus, porphyrins[3] and related ligands (such as sapphyrin[4,5] and triphyrin[6]) act as tridentate ligands toward the $[Re(CO)_3]^+$ fragment to yield unusual "capped" organometallic complexes that obey the 18-electron rule. Likewise, $^{99}Tc(CO)_3$-capped porphyrin derivatives are also well-known.[7] Pentavalent rhenium oxo[8] and rhenium nitrido[9] porphyrins have also been known for decades. The next major developments came in the 1980s in the form of monomeric rhenium(II) porphyrins[10] and metal−metal triple-bonded rhenium(II) porphyrin dimers.[11,12] Rhenium corroles are of more recent provenance: although one was serendipitously isolated some time ago,[13] a general synthetic route to $Re^{V}O$ corroles[14] (as well as to ^{99}TcO corroles[15]) emerged only a few years ago.[16] The simplicity of latter route has also allowed for peripheral functionalization of $Re^{V}O$ corroles via electrophilic aromatic substitution reactions such as halogenation[17] and formylation.[18] Another exciting, recent development has been the synthesis of metal−metal quadruple-bonded rhenium corrole dimers.[19] Detailed electrochemical[20] and density functional theory (DFT)[21] studies of these complexes have yielded a host of new insights into metal−metal quadruple bonding. Herein we provide strong spectroscopic evidence for yet another coordination motif for rhenium in the form of rhenium biscorrole sandwich compounds with the molecular formula ReH[T*p*XPC]$_2$, where T*p*XPC denotes a generic *meso*-tris(*p*-X-phenyl)corrole. One of the corroles in these complexes is thought to be monoprotonated, which results in a seven-coordinate rhenium(V) center.

Rhenium biscorrole sandwich compounds, ReH[T*p*XPC]$_2$, were serendipitously discovered as we attempted to optimize the current synthetic protocol for metal−metal quadruple-bonded rhenium corrole dimers.[19] Heating $Re_2(CO)_{10}$ and free-base corroles H_3[T*p*XPC] (X = H, CH_3, OCH_3) in the presence of a base in 1,2-dichlorobenzene at 150−190 °C resulted in the exclusive formation of Re^{V}[T*p*XPC](O).[14] Increasing the temperature to 190−220 °C resulted in the formation both $Re^{V}O$ corroles and metal−metal quadruple-bonded rhenium corrole dimers {Re[T*p*XPC]}$_2$.[19] Given the clear role of temperature in determining the product profile, we reasoned that the use of even higher temperatures might lead to higher yields of rhenium corrole dimers. Increasing the temperature to 235 °C (*Caution!*), to our surprise, led to yet a third product in addition to $Re^{V}O$ corrole and the rhenium corrole dimer. High-resolution electrospray ionization mass spectrometry (HR-ESI-MS) in the positive mode indicated the molecular formula ReH[T*p*XPC]$_2$ for the new products, which, gratifyingly, could be isolated for each of the three corrole ligands examined (Figure 1).

As for molybdenum and tungsten biscorrole complexes,[22−24] the exceedingly crowded ^{1}H NMR spectra of the new compounds, aside from confirming their diamagnetic nature, proved indecipherable. No hydridic protons were observed, and the NH proton signals in general were also found to be broad and not readily discernible. For one compound, ReH[T*p*OCH$_3$PC]$_2$, natural abundance $^{15}N-^1H$ heteronuclear single quantum coherence did lead to plausible identification of the NH proton to a broad singlet at −0.64 ppm. All three complexes also failed to yield single-crystal X-ray structures. Fortunately, mass spectrometry, optical and X-ray absorption

Received: February 25, 2023
Published: May 23, 2023

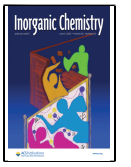

https://doi.org/10.1021/acs.inorgchem.3c00632
Inorg. Chem. 2023, 62, 8467−8471

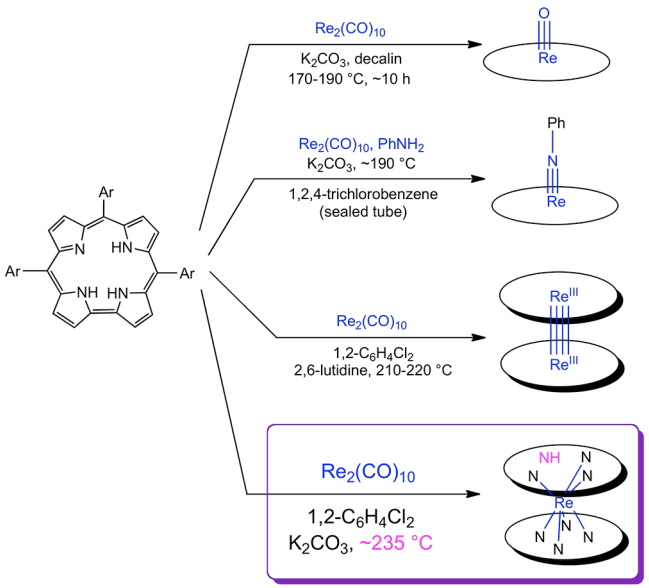

Figure 1. Summary of the interactions between rhenium and corroles as currently elucidated. Inset: this work.

(XAS) spectroscopies, and DFT modeling studies[25−27] paint a fair picture of the structure and nature of the compounds. As for molybdenum and tungsten biscorroles,[22,23] the Soret maxima of ReH[T*p*XPC]$_2$ in dichloromethane and toluene proved to be significantly blue-shifted relative to those of free-base corroles, indirectly lending support to the sandwich formulation (Figure 2). Unusually for electronically innocent metallocorroles,[16] the Soret maxima were found to exhibit significant redshifts with increasing electron-donating character of the substituent X, a behavior typically observed for noninnocent metallocorroles.[27,28] We tentatively ascribe this observation to the unusual geometry of the complex and to charge-transfer character involving the empty Re $5d_{z^2}$ orbital. Upon stirring with 1,8-diazabicyclo[5.4.0]undec-7-ene in anhydrous toluene, the UV−vis spectra sharpened dramatically, consistent with the formation of a C_2-symmetric {Re[T*p*XPC]$_2$}$^-$ anion. The UV−vis spectra of the putative anion are characterized by a deeply split Soret band, with the main feature at ∼438 nm and a prominent, left shoulder at ∼368 nm for X = H and CH_3 and at ∼379 nm for X = OCH_3, again reflecting a significant substituent effect. Importantly, HR-ESI-MS analysis of the putative anions (in methanolic solution) in the negative mode revealed a molecular ion with a mass 1 Da lower than that observed for the neutral compounds (see the Supporting Information).

To determine the most probable location of the "extra" hydrogen in the neutral sandwich compounds, all-electron scalar-relativistic DFT (OLYP[29,30]-D3[31]/ZORA-STO-TZ2P, as implemented in the ADF program system[32]) geometry optimizations were carried out on a variety of potential tautomeric forms of ReH[TPC]$_2$. Assuming an approximate square antiprism of the corrole nitrogens (with the corrole rings rotated approximately 135° relative to each other[22,23]), the global minimum appears to be an nitrogen-protonated tautomer, where the protonated nitrogen belongs to one of the pyrrole rings distal with respect to the direct pyrrole−pyrrole linkage (Figure 3). A rhenium-protonated form could not be located as a local minimum because it spontaneously evolved to the global minimum over the course of the geometry

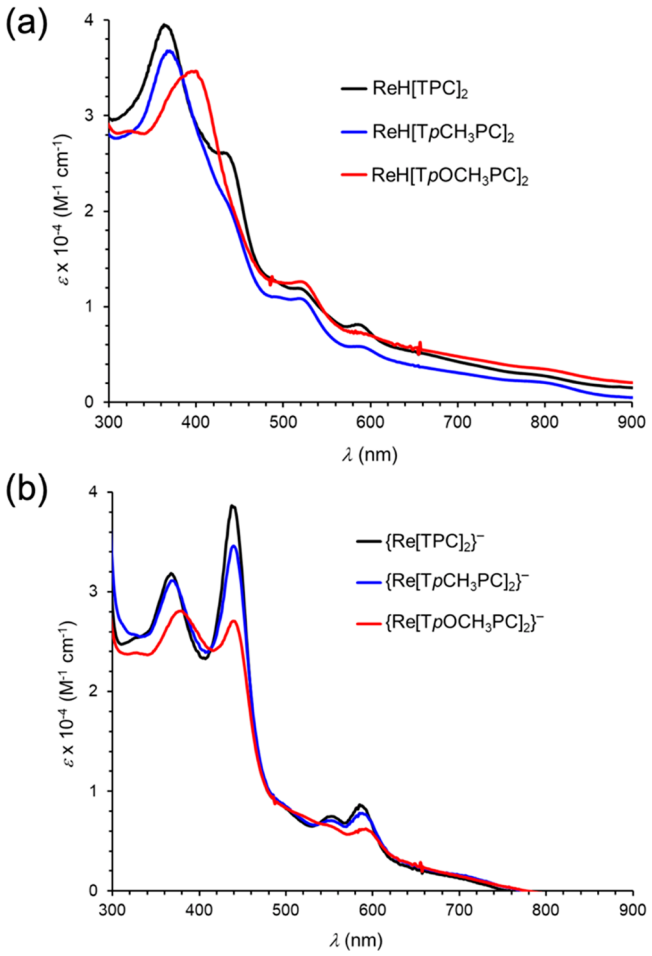

Figure 2. UV−vis spectra of (a) ReH[T*p*XPC]$_2$ and (b) putative {Re[T*p*XPC]$_2$}$^-$ (X = H, CH_3, and OCH_3) anions in anhydrous toluene.

optimization. *meso*-Carbon-protonated forms were also found to be >1.5 eV above the global minimum and so were not considered realistic contenders for the actual structure.

To obtain experimental support for the DFT-derived structure, Re L_3-edge XAS and extended X-ray absorption fine structure (EXAFS) measurements were performed on ReH[TPC]$_2$ (several XAS studies of metalloporphyrins and metallocorroles have been reported in recent years[33−42]). The Re L_3-edge absorption of ReH[TPC]$_2$ was found to be blue-shifted by 2.5 eV relative to the rhenium foil, as assessed by the first derivatives of the absorption features, consistent with the significantly oxidized state of the metal in the complex (Figure S4). The nonphase-shift-corrected EXAFS data (inset), the corresponding Fourier transform, and the best fit are presented in Figure 4. Two qualitative observations may be made from the Fourier transform data: (a) the first shell is split into multiple "subshells" and (b) single- and multiple-scattering contributions from the corrole rings dominate in the ∼2.8−3.2 Å region. FEFF fits to the data reveal a seven-coordinate first shell with 1 Re−N ∼ 1.86 Å, 2 Re−N ∼ 2.37 Å, and 4 Re−N ∼ 2.55 Å (Table 1). The peaks at and below 1 Å in the Fourier transform are artifacts of the background subtraction process in which the normalized XAS data are splined to minimize oscillatory components with periods corresponding to unphysically short metal−ligand bond distances and do not indicate rhenium−ligand backscattering interactions. The longer

https://doi.org/10.1021/acs.inorgchem.3c00632
Inorg. Chem. 2023, 62, 8467−8471

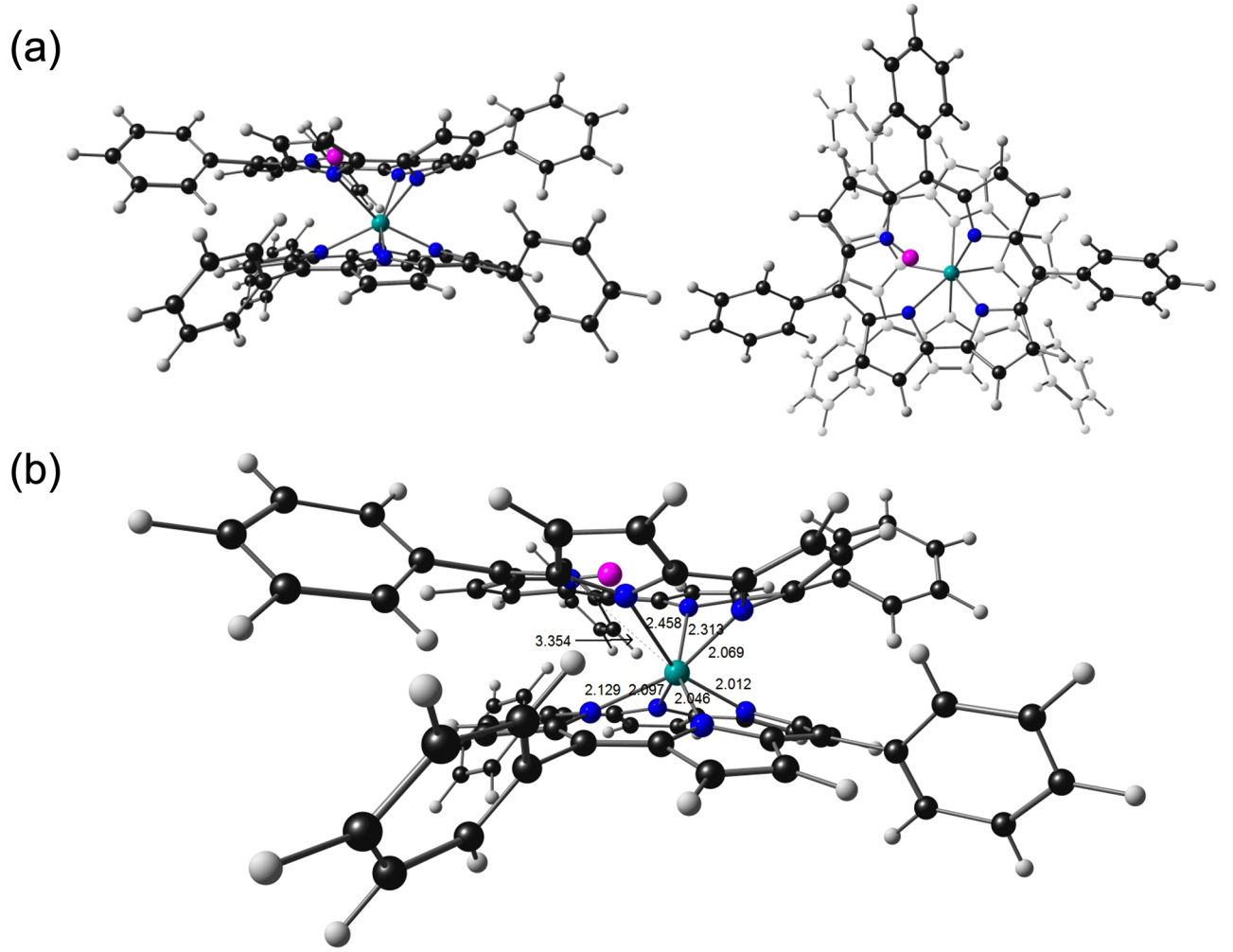

Figure 3. All-electron OLYP-D3/ZORA-STO-TZ2P-optimized geometry of ReH[TPC]$_2$: (a) side and top views; (b) selected distances (Å).

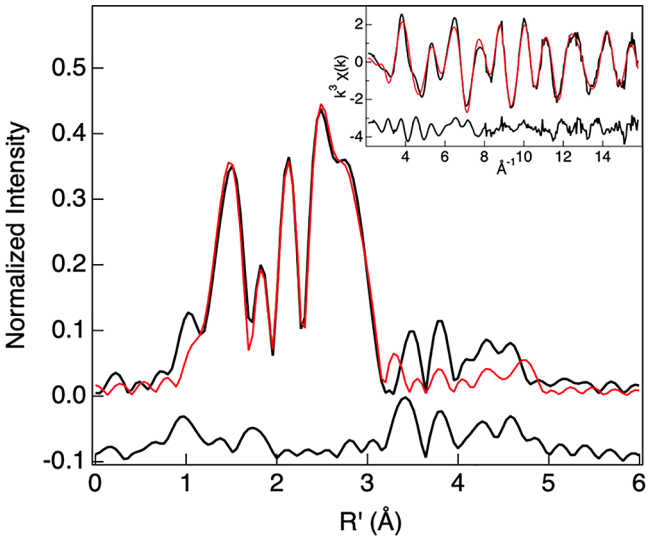

Figure 4. Nonphase-shift-corrected Fourier transforms of the Re L_3-edge EXAFS data for ReH[TPC]$_2$: data (black); fit (red). The inset shows the EXAFS comparison.

distance Re−N paths are correlated with one another and with the Re−C single-scattering contributions from the corrole ligand (Table 1). The Fourier transform intensity in the range

Table 1. EXAFS Least-Squares Fitting Results for ReH[TPC]$_2$

path/shell	R (Å)[a]	σ^2 (Å^2)[b]	ΔE_0 (eV)	F[c]
1 Re−N	1.86	247	−3.40	0.09
2 Re−N	2.37	425		
4 Re−N	2.55	328		
5 Re−C	2.79	637		
10 Re−C−N	3.17	462		
24 Re−C−N	4.93	1475		
24 Re−C−N	5.16	1121		

[a]The estimated standard deviations for the distances are on the order of ±0.02 Å. [b]The σ^2 values are multiplied by 10^5. [c]The error is given by $\sum[(\chi_{obsd} - \chi_{calcd})^2k^6]/\sum[(\chi_{obsd})^2k^6]$. The $S_0{}^2$ factor was set to 1.

R' ∼ 3.2−5.0 Å has multiple contributions from the two corroles. In the fit presented here (Figure 4), this long-range intensity was simulated using two multiple-scattering paths from the corrole (Re−C−N) ring. That said, these paths account for less than 10% of the overall intensity and do not impact the first-shell distances reported in Table 1. Attempts to model the first shell with a total of 8 Re−N distances (split over two or three-shells) resulted in statistically worse fits. The results suggest that ReH[TPC]$_2$ is best described as having a heterogeneous first shell with a total of 7 Re−N interactions.

https://doi.org/10.1021/acs.inorgchem.3c00632
Inorg. Chem. 2023, 62, 8467−8471

In summary, the high-temperature interaction of $Re_2(CO)_{10}$ with three free-base *meso*-triarylcorroles has led to the isolation of neutral rhenium corrole sandwich compounds with the molecular formula ReH[T*p*XPC]$_2$, a heretofore unprecedented coordination motif in the field of rhenium−porphyrinoid interactions.[1,2] DFT calculations and Re L_3-edge EXAFS studies support a seven-coordinate rhenium center and one loosely interacting NH group. The extra hydrogen can be removed by a base, resulting in dramatically sharper UV−vis spectra consistent with C_2-symmetric $\{Re[TpXPC]_2\}^-$ anions. Structural analyses of both the neutral and anionic forms remain a key goal for the future.

■ ASSOCIATED CONTENT

Data Availability Statement

All data generated or analyzed in this study are included in this published article and its Supporting Information.

Supporting Information

The Supporting Information is available free of charge at https://pubs.acs.org/doi/10.1021/acs.inorgchem.3c00632.

Synthetic protocols, HR-ESI-MS and XAS spectra, and DFT-optimized Cartesian coordinates (PDF)

■ AUTHOR INFORMATION

Corresponding Authors

Abhik Ghosh − *Department of Chemistry, University of Tromsø, N-9037 Tromsø, Norway;* orcid.org/0000-0003-1161-6364; Email: abhik.ghosh@uit.no

Ritimukta Sarangi − *Stanford Synchrotron Radiation Lightsource (SSRL), SLAC National Accelerator Laboratory, Stanford University, Menlo Park, California 94025, United States;* orcid.org/0000-0002-2764-2279; Email: ritimukta@gmail.com

Authors

Abraham B. Alemayehu − *Department of Chemistry, University of Tromsø, N-9037 Tromsø, Norway;* orcid.org/0000-0003-0166-8937

Macon Jedediah Abernathy − *Stanford Synchrotron Radiation Lightsource (SSRL), SLAC National Accelerator Laboratory, Stanford University, Menlo Park, California 94025, United States;* orcid.org/0000-0002-0455-2086

Jeanet Conradie − *Department of Chemistry, University of Tromsø, N-9037 Tromsø, Norway; Department of Chemistry, University of the Free State, Bloemfontein 9300, Republic of South Africa;* orcid.org/0000-0002-8120-6830

Complete contact information is available at: https://pubs.acs.org/10.1021/acs.inorgchem.3c00632

Notes

The authors declare no competing financial interest.

■ ACKNOWLEDGMENTS

This work was supported in part by Grant 324139 of the Research Council of Norway (to A.G.) and Grants 129270 and 132504 of South African National Research Foundation (to J.C.). Use of the SSRL, SLAC National Accelerator Laboratory, was supported by the U.S. Department of Energy (DOE), Office of Science, Office of Basic Energy Sciences under Contract DE-AC02-76SF00515. The SSRL Structural Molecular Biology Program is supported by the DOE, Office of Biological and Environmental Research, and by the National Institutes of Health (NIH) and National Institute of General Medical Sciences (NIGMS; P30GM133894). The contents of this publication are solely the responsibility of the authors and do not necessarily represent the official views of NIGMS or NIH.

■ REFERENCES

(1) Chatterjee, T.; Ravikanth, M. 2020. Rhenium complexes of porphyrinoids. *Coord. Chem. Rev.* **2020**, *422*, 213480.

(2) Majumder, S.; Borah, B. P.; Bhuyan, J. Rhenium in the core of porphyrin and rhenium bound to the periphery of porphyrin: synthesis and applications. *Dalton Trans* **2020**, *49*, 8419−8432.

(3) Tsutsui, M.; Ostfeld, D.; Hrung, C. P.; Conway, D. C. Unusual Metalloporphyrins. VII. Porphyrin Bridging Two Metal Atoms: *m*-[mesoporphyrin IX dimethyl esterato]bis[tricarbonylrhenium(I)]. *J. Am. Chem. Soc.* **1971**, *93*, 2548−2549.

(4) Gupta, I.; Srinivasan, A.; Morimoto, T.; Toganoh, M.; Furuta, H. *N*-confused and *N*-fused *meso*-aryl sapphyrins. *Angew. Chem., Int. Ed.* **2008**, *47*, 4563−4567.

(5) Yadav, P.; Fridman, N.; Mizrahi, A.; Gross, Z. Rhenium(I) sapphyrins: remarkable difference between the C_6F_5 and CF_3-substituted derivatives. *Chem. Commun.* **2020**, *56*, 980−983.

(6) Xue, Z. L.; Mack, J.; Lu, H.; Zhang, L.; You, X. Z.; Kuzuhara, D.; Stillman, M.; Yamada, H.; Yamauchi, S.; Kobayashi, N.; Shen, Z. The Synthesis and Properties of Free-Base [14]Triphyrin(2.1.1) Compounds and the Formation of Subporphyrinoid Metal Complexes. *Chem. Eur. J.* **2011**, *17*, 4396−4407.

(7) Tsutsui, M.; Hrung, C. P.; Ostfeld, D.; Srivastava, T. S.; Cullen, D. L.; Meyer, E. F., Jr. Unusual metalloporphyrins. XXIII. Unusual metalloporphyrin complexes of rhenium and technetium. *J. Am. Chem. Soc.* **1975**, *97*, 3952−3965.

(8) Buchler, J. W.; Puppe, L.; Rohbock, K.; Schneehage, H. H. Metall-Komplexe mit Tetrapyrrol-Liganden, VIII. Methoxo-und Phenoxo-metallkomplexe des Octaäthylporphins mit Zentralionen des Typs M^{3+}, M^{4-} und MO^{3-}; neue Wolfram-und Rheniumporphine. *Chem. Ber.* **1973**, *106*, 2710−2732.

(9) Buchler, J. W.; Cian, A. D.; Fischer, J.; Kruppa, S. B.; Weiss, R. Metal complexes with tetrapyrrole ligands, LVII. Synthesis, spectra, and structure of nitridorhenium(V) porphyrins. *Chem. Ber.* **1990**, *123*, 2247−2253.

(10) Collman, J. P.; Garner, J. M.; Kim, K.; Ibers, J. A. Synthesis of Rhenium(II) Porphyrin Complexes and Crystal Structure of Bis-(trimethylphosphine)(tetra-*p*-tolylporphyrinato)rhenium(II)-toluene. *Inorg. Chem.* **1988**, *27*, 4513−4516.

(11) Collman, J. P.; Garner, J. M.; Woo, L. K. The Chemistry of Rhenium and Tungsten Porphyrin Complexes in Low Oxidation States. Synthesis and Characterization of Rhenium and Tungsten Porphyrin Dimers Containing Metal-Metal Multiple Bonds. *J. Am. Chem. Soc.* **1989**, *111*, 8141−8148.

(12) Collman, J. P.; Arnold, H. J. Multiple Metal-Metal Bonds in 4d and 5d Metal-Porphyrin Dimers. *Acc. Chem. Res.* **1993**, *26*, 586−592.

(13) Tse, M. K.; Zhang, Z.; Chan, K. S. Synthesis of an Oxorhenium(V) Corrolate from Porphyrin with Detrifluoromethylation and Ring Contraction. *Chem. Commun.* **1998**, 1199−1200.

(14) Einrem, R. F.; Gagnon, K. J.; Alemayehu, A. B.; Ghosh, A. Metal-Ligand Misfits: Facile Access to Rhenium-Oxo Corroles by Oxidative Metalation. *Chem. Eur. J.* **2016**, *22*, 517−520.

(15) Einrem, R. F.; Braband, H.; Fox, T.; Vazquez-Lima, H.; Alberto, R.; Ghosh, A. Synthesis and Molecular Structure of ^{99}Tc Corroles. *Chem. Eur. J.* **2016**, *22*, 18747−18751.

(16) Alemayehu, A. B.; Thomas, K. E.; Einrem, R. F.; Ghosh, A. The Story of 5d Metallocorroles: From Metal−Ligand Misfits to New Building Blocks for Cancer Phototherapeutics. *Acc. Chem. Res.* **2021**, *54*, 3095−3107.

(17) Alemayehu, A. B.; Einrem, R. F.; McCormick-McPherson, L. J.; Settineri, N. S.; Ghosh, A. Synthesis and molecular structure of perhalogenated rhenium-oxo corroles. *Sci. Rep.* **2020**, *10*, 19727.

(18) Einrem, R. F.; Jonsson, E. T.; Teat, S. J.; Settineri, N. S.; Alemayehu, A. B.; Ghosh, A. Regioselective formylation of rhenium-oxo and gold corroles: substituent effects on optical spectra and redox potentials. *RSC Adv.* **2021**, *11*, 34086−34094.
(19) Alemayehu, A. B.; McCormick-McPherson, L. J.; Conradie, J.; Ghosh, A. Rhenium Corrole Dimers: Electrochemical Insights into the Nature of the Metal−Metal Quadruple Bond. *Inorg. Chem.* **2021**, *60*, 8315−8321.
(20) Osterloh, W. R.; Conradie, J.; Alemayehu, A. B.; Ghosh, A.; Kadish, K. M. The Question of the Redox Site in Metal−Metal Multiple-Bonded Metallocorrole Dimers. *ACS Org. Inorg. Au* **2023**, *3*, 35−40.
(21) Conradie, J.; Vazquez-Lima, H.; Alemayehu, A. B.; Ghosh, A. 2021. Comparing Isoelectronic, Quadruple-Bonded Metalloporphyrin and Metallocorrole Dimers: Scalar-Relativistic DFT Calculations Predict $a > 1$ eV Range for Ionization Potential and Electron Affinity. *ACS Physical Chemistry Au* **2022**, *2*, 70−78.
(22) Alemayehu, A. B.; Vazquez-Lima, H.; Gagnon, K. J.; Ghosh, A. Tungsten Biscorroles: New Chiral Sandwich Compounds. *Chem. Eur. J.* **2016**, *22*, 6914−6920.
(23) Alemayehu, A. B.; Vazquez-Lima, H.; McCormick, L. J.; Ghosh, A. Relativistic effects in metallocorroles: comparison of molybdenum and tungsten biscorroles. *Chem. Commun.* **2017**, *53*, 5830−5833.
(24) Schies, C.; Alemayehu, A. B.; Vazquez-Lima, H.; Thomas, K. E.; Bruhn, T.; Bringmann, G.; Ghosh, A. Metallocorroles as inherently chiral chromophores: resolution and electronic circular dichroism spectroscopy of a tungsten biscorrole. *Chem. Commun.* **2017**, *53*, 6121−6124.
(25) Ghosh, A. Just how good is DFT? *J. Biol. Inorg. Chem.* **2006**, *11*, 671−673.
(26) Thomas, K. E.; Alemayehu, A. B.; Conradie, J.; Beavers, C. M.; Ghosh, A. The Structural Chemistry of Metallocorroles: Combined X-Ray Crystallography and Quantum Chemistry Studies Afford Unique Insights. *Acc. Chem. Res.* **2012**, *45*, 1203−1214.
(27) Ghosh, A. Electronic Structure of Corrole Derivatives: Insights from Molecular Structures, Spectroscopy, Electrochemistry, and Quantum Chemical Calculations. *Chem. Rev.* **2017**, *117*, 3798−3881.
(28) Ganguly, S.; Ghosh, A. Seven Clues to Ligand Noninnocence: The Metallocorrole Paradigm. *Acc. Chem. Res.* **2019**, *52*, 2003−2014.
(29) Handy, N. C.; Cohen, A. J. Left-right correlation energy. *Mol. Phys.* **2001**, *99*, 403−412.
(30) Lee, C.; Yang, W.; Parr, R. G. Development of the Colle-Salvetti correlation-energy formula into a functional of the electron density. *Phys. Rev. B* **1988**, *37*, 785−789.
(31) Grimme, S.; Antony, J.; Ehrlich, S.; Krieg, H. A Consistent and Accurate *Ab Initio* Parametrization of Density Functional Dispersion Correction (DFT-D) for the 94 Elements H-Pu. *J. Chem. Phys.* **2010**, *132*, 154104.
(32) te Velde, G. T.; Bickelhaupt, F. M.; Baerends, E. J.; Fonseca Guerra, C.; van Gisbergen, S. J. A.; Snijders, J. G.; Ziegler, T. Chemistry with ADF. *J. Comput. Chem.* **2001**, *22*, 931−967.
(33) Hocking, R. K.; Wasinger, E. C.; Yan, Y. L.; Degroot, F. M.; Walker, F. A.; Hodgson, K. O.; Hedman, B.; Solomon, E. I. Fe L-edge X-ray Absorption Spectroscopy of Low-Spin Heme Relative to Non-Heme Fe Complexes: Delocalization of Fe d-Electrons into the Porphyrin Ligand. *J. Am. Chem. Soc.* **2007**, *129*, 113−125.
(34) Hocking, R. K.; George, S. D.; Gross, Z.; Walker, F. A.; Hodgson, K. O.; Hedman, B.; Solomon, E. I. Fe L-and K-edge XAS of Low-Spin Ferric Corrole: Bonding and Reactivity Relative to Low-Spin Ferric Porphyrin. *Inorg. Chem.* **2009**, *48*, 1678−1688.
(35) Wilson, S. A.; Kroll, T.; Decreau, R. A.; Hocking, R. K.; Lundberg, M.; Hedman, B.; Hodgson, K. O.; Solomon, E. I. Iron L-Edge X-ray Absorption Spectroscopy of Oxy-Picket Fence Porphyrin: Experimental Insight into Fe−O_2 Bonding. *J. Am. Chem. Soc.* **2013**, *135*, 1124−1136.
(36) Sarangi, R.; Giles, L. J.; Thomas, K. E.; Ghosh, A. Ligand Noninnocence in Silver Corroles: A XANES Investigation. *Eur. J. Inorg. Chem.* **2016**, *2016*, 3225−3227.
(37) Ganguly, S.; Giles, L. J.; Thomas, K. E.; Sarangi, R.; Ghosh, A. Ligand Noninnocence in Iron Corroles: Insights from Optical and X-ray Absorption Spectroscopies and Electrochemical Redox Potentials. *Chem. Eur. J.* **2017**, *23*, 15098−15106.
(38) Ganguly, S.; Renz, D.; Giles, L. J.; Gagnon, K. J.; McCormick, L. J.; Conradie, J.; Sarangi, R.; Ghosh, A. Cobalt- and Rhodium-Corrole-Triphenylphosphine Complexes Revisited: the Question of a Noninnocent Corrole. *Inorg. Chem.* **2017**, *56*, 14788−14800.
(39) Ganguly, S.; McCormick, L. J.; Conradie, J.; Gagnon, K. J.; Sarangi, R.; Ghosh, A. Electronic Structure of Manganese Corroles Revisited: X-ray Structures, Optical and X-ray Absorption Spectroscopies, and Electrochemistry as Probes of Ligand Noninnocence. *Inorg. Chem.* **2018**, *57*, 9656−9669.
(40) Lim, H.; Thomas, K. E.; Hedman, B.; Hodgson, K. O.; Ghosh, A.; Solomon, E. I. X-ray Absorption Spectroscopy as a Probe of Ligand Noninnocence in Metallocorroles: The Case of Copper Corroles. *Inorg. Chem.* **2019**, *58*, 6722−6730.
(41) Cao, R.; Thomas, K. E.; Ghosh, A.; Sarangi, R. X-ray absorption spectroscopy of archetypal chromium porphyrin and corrole derivatives. *RSC Adv.* **2020**, *10*, 20572−20578.
(42) Matson, B. D.; Thomas, K. E.; Alemayehu, A. B.; Ghosh, A.; Sarangi, R. X-ray absorption spectroscopy of exemplary platinum porphyrin and corrole derivatives: metal-versus ligand-centered oxidation. *RSC Adv.* **2021**, *11*, 32269−32274.

https://doi.org/10.1021/acs.inorgchem.3c00632
Inorg. Chem. 2023, 62, 8467−8471